Biophysical Reports

LETTER

Characteristic energy scales of active fluctuations in adherent cells

Avraham Moriel,[1] Haguy Wolfenson,[2] and Eran Bouchbinder[1,*]

[1]Chemical and Biological Physics Department, Weizmann Institute of Science, Rehovot, Israel and [2]Department of Genetics and Developmental Biology, Rappaport Faculty of Medicine, Technion-Israel Institute of Technology, Haifa, Israel

ABSTRACT Cell-matrix and cell-cell adhesion play important roles in a wide variety of physiological processes, from the single-cell level to the large scale, multicellular organization of tissues. Cells actively apply forces to their environment, either extracellular matrix or neighboring cells, as well as sense its biophysical properties. The fluctuations associated with these active processes occur on an energy scale much larger than that of ordinary thermal equilibrium fluctuations, yet their statistical properties and characteristic scales are not fully understood. Here, we compare measurements of the energy scale of active cellular fluctuations—an effective cellular temperature—in four different biophysical settings, involving both single-cell and cell-aggregate experiments under various control conditions, different cell types, and various biophysical observables. The results indicate that a similar energy scale of active fluctuations might characterize the same cell type in different settings, though it may vary among different cell types, being approximately six to eight orders of magnitude larger than the ordinary thermal energy at room temperature. These findings call for extracting the energy scale of active fluctuations over a broader range of cell types, experimental settings, and biophysical observables and for understanding the biophysical origin and significance of such cellular energy scales.

WHY IT MATTERS Fluctuations play important roles in many physiological processes, ranging from the interactions of individual cells with their microenvironment to the development of tissues. Yet, due to their active, out of thermal equilibrium nature, these fluctuations are rather poorly characterized and understood. We show that active fluctuations in adherent cells—related to both cell-microenvironment and cell-cell adhesions—can be characterized by an effective temperature (a characteristic energy scale) that is six to eight orders of magnitude larger than the ambient temperature. These findings open the way for more systematic and quantitative analyses of active fluctuations in adherent cells and tissues, and also highlight the need to extend such analyses to a broader range of biophysical settings and cell/tissue types.

INTRODUCTION

Noise and fluctuations play important roles in a wide variety of natural and man-made systems. In thermal equilibrium, thermal fluctuations are accurately described by equilibrium statistical thermodynamics and are controlled by the ambient temperature. Quenched noise, i.e., fluctuations and inhomogeneity in the system's structure, is also of great importance. In living systems, which are of active nature absent in inanimate matter and which are intrinsically out of equilibrium, fluctuations are also highly relevant, yet are far less characterized and understood. In this letter, we discuss the quantification of characteristic energy scales of active fluctuations (and in some cases, their statistical distributions) in adherent cells based on four different experimental settings, various biophysical observables, and several cell types. Such fluctuations are important for a wide variety of physiological processes, from the single-cell level to the multicellular organization of tissues, and their quantification is expected to significantly affect our fundamental understanding of these processes.

RESULTS

Here, we describe and discuss measurements of characteristic energy scales of active fluctuations in adherent cells, adhering either to an extracellular

Submitted August 18, 2022, and accepted for publication December 23, 2022.

*Correspondence: eran.bouchbinder@weizmann.ac.il

Editor: Jorg Enderlein.

https://doi.org/10.1016/j.bpr.2022.100099

matrix or to other cells, in four experimental settings and including six cell types in total. Two of the experimental settings are our own, and two are related to works available in the literature.

Cell-scale orientational fluctuations of noninteracting cells under periodic forcing

In various physiological situations, cells are exposed to high-frequency periodic driving forces in addition to intrinsic and extrinsic noise, e.g., in vital conditions encountered in cardiovascular tissues in hemodynamic environments, in the lungs under breathing motion, and in cardiac tissue under rhythmic heart beating. Numerous well-controlled laboratory experiments, in which living cells adhere to a deformable substrate experiencing periodic driving forces (see, for example, (1–10)), revealed that under such conditions, cells reorient themselves to well-defined angles.

In such experiments, cells are exposed to a time-dependent strain tensor $\boldsymbol{\varepsilon}(t)$ of the form $\boldsymbol{\varepsilon}(t) = \frac{1}{2}\begin{pmatrix} \epsilon & 0 \\ 0 & -r\epsilon \end{pmatrix}[1 - \cos(2\pi f t)]$, where ϵ is the strain amplitude in the principal direction, $-r\epsilon$ is the strain amplitude in the perpendicular direction, and r is the biaxiality strain ratio, cf. Fig. 1 *a*. The experimentalist externally controls ϵ, r, and the periodic forcing frequency f (typically in the physiologically relevant range of ~ 1 Hz) and tracks the time evolution of the orientation of individual cells, $\theta(t)$. In (9), it has been shown that $\theta(t)$ is quantitatively predicted by $\dot{\theta}(t) = -\tau^{-1} d\overline{u}(\theta)/d\theta$, where $\overline{u}(\theta)$ is a dimensionless cellular elastic energy that depends on the instantaneous orientation $\theta(t)$ relative to the principal strain direction. It is given by $\overline{u}(\theta) = \frac{1}{2}\epsilon^2[b^{-1}(1+r)\cos^2(\theta) - b^{-1} + (1-r)]^2$, where b is a dimensionless number that quantifies the elastic anisotropy of the cell (9,10). Finally, τ is a cellular timescale that is related to active remodeling. The dynamical equation that quantitatively describes $\theta(t)$, written above, is an out-of-equilibrium one, involving both rapidly varying external forces and active cellular processes.

Recently (10,11), the out-of-equilibrium, dynamical equation for $\theta(t)$ has been extended to include stochastic effects on cellular orientation by assuming the existence of an additive, uncorrelated noise of yet-unknown amplitude (see also (11)). The resulting out-of-equilibrium Langevin equation can be then transformed into a Fokker-Planck equation for the time evolution of the probability distribution function $p(\theta, t)$ of an ensemble of noninteracting cells (12). After applying the periodic forces for sufficiently long time t (the theory of (9) shows that t should be sufficiently larger than $\epsilon^{-2}\tau$), $p(\theta, t)$ approaches a stationary distribution, to be denoted by $p(\theta)$. A stationary state of an ensemble of noninteracting fibroblasts (REF-52) is shown in Fig. 1 *a*, where cells are oriented predominantly along one of two mirror-image angles, with some fluctuations. In Fig. 1 *b*, we present one of the oriented cells, whose focal adhesions (*green*) and stress fibers (*red*) are colored.

The stationary probability distribution function $p(\theta)$ has been recently predicted (9,10,12) to take the form

$$p(\theta) \sim \exp\left(-\frac{U(\theta)}{k_B T_{\text{eff}}}\right). \tag{1}$$

Here, $U(\theta) = \frac{1}{2}V_{\text{cell}}E_{\text{cell}}\epsilon^2[b^{-1}(1+r)\cos^2(\theta) - b^{-1} + (1-r)]^2 = V_{\text{cell}}E_{\text{cell}}\overline{u}(\theta)$, where $\overline{u}(\theta)$ was presented above in the context of the reorientation dynamics, V_{cell} is the volume of the cell, and E_{cell} is its coarse-grained elastic modulus. T_{eff} is an effective temperature associated with active orientational fluctuations, which is proportional to the yet-unknown amplitude of the additive noise, and k_B is Boltzmann's constant. It is important to note that we adopt the symbols $k_B T_{\text{eff}}$ and the term "effective temperature" since they have been used in previous works in a related context (4,13). In so doing, we do not insist on the existence of generalized thermodynamics of adherent cells; $k_B T_{\text{eff}}$ just represents a characteristic energy scale of fluctuations that we aim at determining.

The probability density $p(\theta)$ in Eq. 1 is theoretically predicted up to the unknown dimensionless combination $(k_B T_{\text{eff}})/(V_{\text{cell}}E_{\text{cell}})$ (10), which can be then extracted from experiments. This quantitative comparison to experiments has been pursued very recently in (10) and revealed favorable agreement; a few examples are reported here. In Fig. 1 *c*, we present $p(\theta)$ for rat embryo fibroblasts (REF-52, the experimental data correspond to Fig. 3 *b* in (10)). The solid line corresponds to the theoretical prediction in Eq. 1 obtained with a single parameter fit, yielding $(k_B T_{\text{eff}})/(V_{\text{cell}}E_{\text{cell}}) = 3.2 \times 10^{-5}$. In order to transform the latter into an effective temperature in physical units, we need estimates of V_{cell} and E_{cell}. The area of the REF-52 shown in Fig. 1 *b* is roughly 3,000 μm^2 and its height is about 2 μm, leading to $V_{\text{cell}} \approx 6 \times 10^{-15}$ m^3 (note that V_{cell} is likely to reveal cell-cell variability and follow its own statistical distribution, which is not taken into account here). The coarse-grained elastic modulus of REF-52 under these biophysical conditions was estimated to be $E_{\text{cell}} \approx 10$ kPa (10). Taken together, we obtain $T_{\text{eff}} \sim 10^8$ K, which is about six orders of magnitude larger than room temperature.

Our next goal is to see whether and to what extent T_{eff} might differ for different cell types under

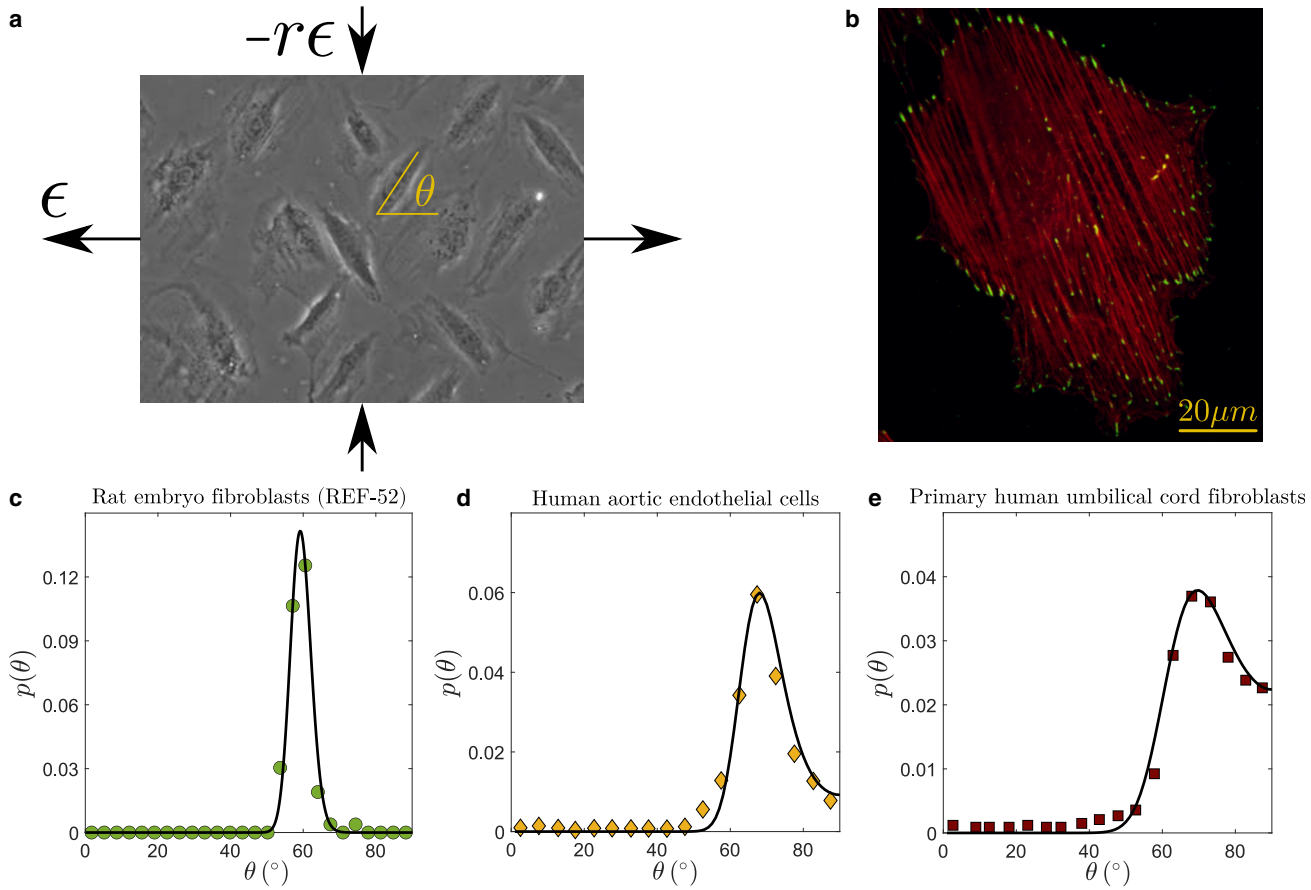

FIGURE. 1 (*a*) A top view of REF-52 cells on a PDMS substrate under long-time periodic loading with principal strain amplitude of ϵ, biaxiality ratio r (both illustrated on the figure), and frequency f; see text for additional details. The cells, which initially featured random orientations, are all approximately oriented at an angle θ (relative to the principal strain direction, marked on the figure) or its mirror-image angle $-\theta$ (not marked) in the long-time limit. (*b*) A zoom in on a single REF-52 in its oriented state (after 6 h of periodic stretching), showing its stress fibers (*red*) and focal adhesions (*green*) (10). The scale bar represents 20 μm. (*c*) Measured $p(\theta)$ for REF-52 (*green circles*) under long-time periodic stretching with $\epsilon = 10.4\,\%$, $r = 0.46$, and $f = 1.2$ Hz (adapted from Fig. 3 *b* of (10)).The solid line corresponds to Eq. 1, with $b = 1.15$ extracted from the maximum of the distribution (see main text for details) and a single fitting parameter set to $(k_B T_{eff})/(V_{cell} E_{cell}) = 3.2 \times 10^{-5}$. (*d*) Measured $p(\theta)$ for human aortic endothelial cells (*orange diamonds*) under periodic stretching with $\epsilon = 10.0\%$, $r = 0.34$, and $f = 0.5$ Hz (see Fig. 5 *b* in (5) and Fig. 3 *a* in (10)). The solid line corresponds to Eq. 1, with $b = 1.23$ extracted from the maximum of the distribution (see main text for details) and a single fitting parameter set to $(k_B T_{eff})/(V_{cell} E_{cell}) = 6.2 \times 10^{-5}$. (*e*) Measured $p(\theta)$ for primary human umbilical cord fibroblasts (*brown squares*) under periodic stretching with $\epsilon = 31.7\%$, $r = 0.28$, and $f = 9 \times 10^{-3}$ Hz (see Fig. 4 in (4) and Fig. 2 f in (10)). The solid line corresponds to Eq. 1, with $b = 1.18$ extracted from the maximum of the distribution and a single fitting parameter set to $(k_B T_{eff})/(V_{cell} E_{cell}) = 1.6 \times 10^{-3}$.

approximately the same biophysical conditions. In Fig. 1 *d*, we present $p(\theta)$ for human aortic endothelial cells under similar periodic driving conditions (the experimental data correspond to Fig. 3a in (10), which were extracted from Fig. 5B in (5)). The solid line corresponds to the theoretical prediction in Eq. 1 obtained with a single parameter fit (see the values of the other known parameters in the figure caption), yielding $(k_B T_{eff})/(V_{cell} E_{cell}) = 6.2 \times 10^{-5}$, a similar dimensionless value as the one obtained for REF-52. Assuming that V_{cell} and E_{cell} are roughly similar to the corresponding values of REF-52, we conclude that the two cell types feature roughly the same T_{eff} under similar biophysical conditions.

To further test the degree of generality of this interesting result, we present in Fig. 1 *e* $p(\theta)$ for primary human umbilical cord fibroblasts under similar periodic driving conditions (the experimental data correspond to Fig. 2 f in (10), which were extracted from Fig. 4 in (4)). The solid line corresponds to the theoretical prediction in Eq. 1 obtained with a single parameter fit (see the values of the known parameters in the figure caption), yielding $(k_B T_{eff})/(V_{cell} E_{cell}) = 1.6 \times 10^{-3}$. Assuming again that V_{cell} and E_{cell} are roughly similar to the corresponding values of the two other cell types considered above, one obtains $T_{eff} \sim 10^{10}$ K, which is about two orders of magnitude larger than the value estimated for the two other cell types considered

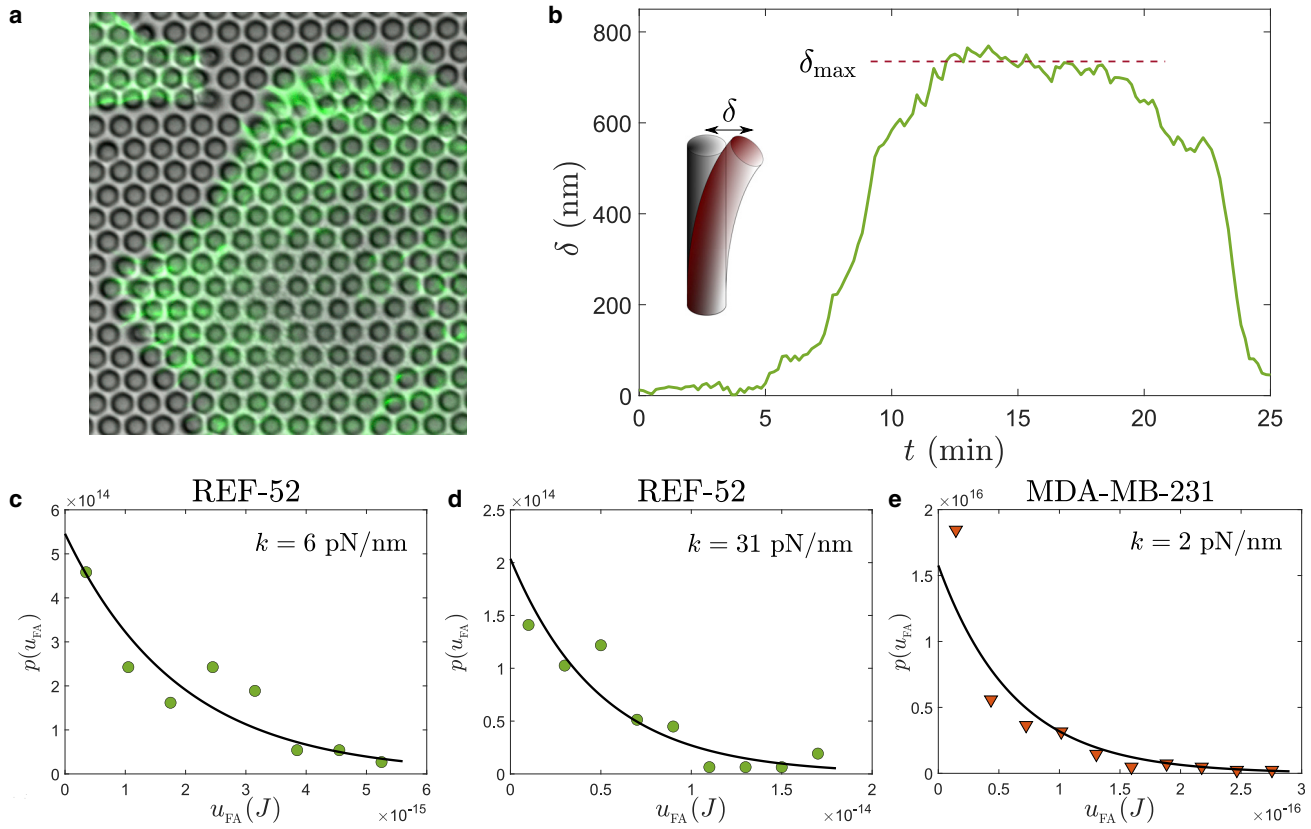

FIGURE. 2 (*a*) A top view of a REF-52 cell, whose F-actin is shown in green, adhering to a micropillar array (the micropillar's diameter is 2 μm and the pillars center-to-center distance is 4 μm) in its steady spreading state (a portion of another REF-52 is observed at the top left corner). (*b*) An example of a displacement δ of a micropillar (here of bending rigidity $k = 31$ pN/nm) as a function of time t in the steady spreading state. The displacement (deflection) δ is illustrated in the inset (the magnitude of δ is exaggerated for visual clarify). Here, $t = 0$ is chosen such that the buildup of force/displacement as a focal adhesion starts to assemble around $t = 5$ min is observed. $\delta(t)$ reaches a maximal displacement $\delta_{\max}$ (marked on the figure), where it plateaus for ~ 10 min, before the focal adhesion starts to disassemble, until the micropillar is released around $t = 25$ min. (*c*) Measured $p(u_{\mathrm{FA}})$ for REF-52 (*green circles*), where $u_{\mathrm{FA}} \equiv \frac{1}{2} k \delta^2_{\max}$, with $k = 6$ pN/nm. The solid line corresponds to Eq. 2 with a single fitting parameter set to $T_{\mathrm{eff}} = 1.4 \times 10^8$ K. (*d*) The same as (*c*) but for $k = 31$ pN/nm. The solid line corresponds to Eq. 2 with a single fitting parameter set to $T_{\mathrm{eff}} = 3.6 \times 10^8$ K. (*e*) Measured $p(u_{\mathrm{FA}})$ for human breast adenocarcinoma cells (MDA-MB-231, orange triangles), with $k = 2$ pN/nm. The solid line corresponds to Eq. 2 with a single fitting parameter set to $T_{\mathrm{eff}} = 4.5 \times 10^6$ K.

above (and about eight orders of magnitude larger than room temperature). Interestingly, it has been recently shown that primary human umbilical cord fibroblasts feature a dramatically different intrinsic timescale τ (related to reorientation dynamics discussed above) compared with REF-52 (10). It would be interesting to explore in future work whether this difference is related to the enhanced level of fluctuations they exhibit. One way or the other, the results indicate that T_{eff} might be cell-type dependent and is always many orders of magnitude larger than room temperature.

Adhesion-scale contractile energy fluctuations of stationary adherent cells

Our next goal is to test whether the same cell type features the same characteristic energy scale of fluctuations, quantified by T_{eff}, under different biophysical settings and observables under consideration. To that aim, we consider REF-52 cells adhering to an array of fibronectin-coated, flexible, polydimethylsiloxane (PDMS) micropillars (14), cf. Fig. 2 *a*, without applying external driving forces. The micropillars resist deflection according to the Euler-Bernoulli beam theory, featuring bending rigidity $k = 3\pi E R^4 H^{-3}/4$, where R is the pillar's radius, H is the pillar's height, and E is the Young's modulus of PDMS (see the caption of Fig. 2 for the values of R and k, as well as for the micropillar center-to-center distance).

The cells are allowed to adhere to the micropillar array for a sufficiently long period of time, until they reach a steady spreading state. The latter steady state, where the cell features a constant area on average, is still subjected to fluctuations. In particular,

in the steady spreading state, focal adhesions are formed at micropillars and apply to them a contractile force, resulting in a displacement of magnitude $\delta(t)$ as a function of time t. As shown in Fig. 2 *b*, $\delta(t)$ initially rises and reaches a characteristic maximal value $\delta_{\max}$, and after leveling off for a characteristic time of 10 min, it decreases until the focal adhesion disassembles altogether and reassembles at a nearby micropillar (the latter is not shown).

We then define a characteristic adhesion-scale contractile energy as $u_{\mathrm{FA}} \equiv \frac{1}{2} k \delta_{\max}^2$, where the subscript FA stands for focal adhesion. It is important to note that u_{FA} is a contractile energy defined at the single FA scale (i.e., it characterizes the energy the cell invests in deflecting a single pillar through a single FA) and generated by the cell, as opposed to $U(\theta)$ of Eq. 1, which is a cell-scale elastic energy related to the external driving force.

Considering an ensemble of noninteracting cells in the steady spreading state, i.e., accounting for both intracell and intercell variations, we construct the probability distribution function $p(u_{\mathrm{FA}})$, presented in Fig. 2 *c* for a micropillar array with $k = 6$ pN/nm. We find, empirically, that the measured distributions can be approximately described by the following form

$$p(u_{\mathrm{FA}}) \sim \exp\left(-\frac{u_{\mathrm{FA}}}{k_{\mathrm{B}} T_{\mathrm{eff}}}\right), \tag{2}$$

which readily allows us to extract the characteristic energy fluctuations scale $k_{\mathrm{B}} T_{\mathrm{eff}}$ in its natural physical units. The latter is a clear advantage as it does not involve the uncertainties associated with V_{cell} and E_{cell}, which were required in the previous subsection in order to transform a dimensionless effective temperature to a dimensional one. A Boltzmann-like fit of Eq. 2 with $T_{\mathrm{eff}} = 1.4 \times 10^8$ K is added to Fig. 2 *c* in the solid line. Quite remarkably, $T_{\mathrm{eff}} = 1.4 \times 10^8$ K coincides with the value of T_{eff} extracted in Fig. 1 *c* for the same cell type, but for a different biophysical setting and a different probed observable. This result suggests that a similar energy scale of fluctuations may characterize the same cell type in different situations, a possibility that clearly calls for additional investigation.

To further look into this issue, we present in Fig. 1 *d* $p(u_{\mathrm{FA}})$ for REF-52 in exactly the same experimental setting as in Fig. 1 *c* but for a fivefold larger micropillar bending rigidity, i.e., $k = 31$ pN/nm. It is crucial to stress that the substrate rigidity is varied by geometry; k in this experimental paradigm is varied by varying the micropillar height H alone, keeping its radius R, the substrate modulus E (here of PDMS), and the surface chemistry (here the fibronectin coating) fixed; this is one of the greatest advantages of the micropillar array paradigm (14). The distribution is again Boltzmann-like and fit to Eq. (2), with $T_{\mathrm{eff}} = 3.6 \times 10^8$ K, was added to Fig. 2 *d* in the solid line. While this T_{eff} is not fivefold different from that of the $k = 6$ pN/nm value, it clearly indicates that the energy scale of fluctuations is not an entirely intrinsic property.

All of the cell types considered above form rather strong adhesions and apply significant forces to the extracellular matrix—through stress fibers—or to each other—through cell-cell bonds. It would be thus interesting to consider yet another cell type that is known to attach weakly to the microenvironment and to posses few force-generating stress fibers. In this case, we expect T_{eff} to be significantly smaller. To that aim, we consider human breast adenocarcinoma cells MDA-MB-231 (an epithelial human breast cancer cell line), which is a model cell line for invasive cancer. These cells are very motile and possess very few stress fibers, if at all (see, for example, (15)). We apply the same experimental paradigm to MDA-MB-231 using a micropillar array with $k = 2$ pN/nm. The results are presented in Fig. 2 *e*, where a Boltzmann-like fit of Eq. 2 with $T_{\mathrm{eff}} = 4.5 \times 10^6$ K is added in the solid line. This T_{eff} value is $\sim$2 orders of magnitude smaller than the values obtained for REF-52 under similar conditions, in agreement with our expectation. Finally, note that for all three cell types considered in Fig. 2, *c*–*e*, the standard deviation of the distribution—quantified by $k_{\mathrm{B}} T_{\mathrm{eff}}$—is comparable to its mean $\langle u_{\mathrm{FA}} \rangle$, an observation that might be of importance for cellular and tissue dynamics.

We stress that the Boltzmann-like expression for $p(u_{\mathrm{FA}})$ in Eq. 2 differs from $p(\theta)$ of Eq. 1 in several important respects. First, the latter depends on a cell-scale elastic energy $U(\theta)$, while the former depends on an adhesion-scale contractile energy u_{FA}, which is directly measured. Second, the biophysical situation related to Eq. 1 involves external driving forces, while that of Eq. 2 does not (rather, fluctuations emerge entirely from cellular active contractility at the single adhesion scale). Finally, Eq. 1 is a theoretical prediction, while Eq. 2 is an empirical fit, i.e., an experimental observation.

Energy fluctuations of a single cell moving inside an aggregate of other cells

Next, we briefly consider a different set of experiments available in the literature, where T_{eff} is also estimated. In (16), the motion of individual pigmented retinal epithelial cells in aggregates of neural retinal cells (obtained from chicken embryos) has been tracked. The individual cells undergo a random walk, characterized by a linear diffusion coefficient $D \simeq 3 \times 10^{-12}$ cm^2/s $= 3 \times 10^{-16}$ m^2/s (16). The viscosity of the

aggregate was measured to be $\eta \simeq 10^5$ Pa• s (17). Then, assuming an equilibrium-like Stokes-Einstein relation for the linear diffusion of one liquid inside another of the form $T_{\text{eff}} = 5\pi D\eta a/(2k_{\text{B}})$ (this is a standard relation, see (17) for references) yielded an estimate of $T_{\text{eff}} \simeq 1.4 \times 10^8$ K using $a \simeq 8$ μm for the linear dimension of the cell (17). Very interestingly, this energy scale of fluctuations roughly coincides with the T_{eff} obtained for REF-52 and human aortic endothelial cells in very different biophysical situations.

It is important to note that the literature measurements and analysis of a single cell moving inside an aggregate of other cells briefly mentioned here invoked an equilibrium-like relation (where the ordinary temperature is replaced by an effective temperature T_{eff}) based on an analogy to the linear diffusion of one liquid inside another. No such equilibrium-like relations have been invoked in our own analyses discussed in "*cell-scale orientational fluctuations of noninteracting cells under periodic forcing*" and "*adhesion-scale contractile energy fluctuations of stationary adherent cells*".

Interfacial energy fluctuations during cell sorting in a mixture of two cell-type aggregates

Experiments related to those briefly reported in the previous subsection studied cell sorting in a mixture of the same two types of cells (i.e., pigmented retinal epithelial cells and neural retinal cells (17)). Employing an analogy between cell sorting and the separation of immiscible fluids allowed to extract an energy fluctuations scale characterizing the interface between two cell aggregates.

For two immiscible fluids at thermal equilibrium, the ordinary temperature T is related to the interfacial tension σ_{t} through $T = \frac{\langle z^2 \rangle \sigma_{\text{t}}}{k_{\text{B}} \ln(L/a)}$ in two dimensions (this is a standard relation, see (17) for references). Replacing T with T_{eff} and using the measured mean-squared displacement $\langle z^2 \rangle \simeq 0.04a^2$ perpendicular to the interface (i.e., $\langle z^2 \rangle$ is a measure of interfacial tissue fluctuations, where $\langle \bullet \rangle$ is an average over the entire interfacial area), the measured neural retina-pigmented epithelium interfacial tension $\sigma_{\text{t}} \simeq 10$ dyne/cm $= 10^{-2}$ N/m, the measured linear size of the pigmented epithelial cell aggregate $L \simeq 200$ μm, and the measured linear dimension of the cell $a \simeq 8$ μm (as in the previous subsection), one obtains $T_{\text{eff}} \simeq 5.8 \times 10^8$ K.

This value of T_{eff} is in the same ballpark as the one obtained in the previous subsection, which also coincides with the T_{eff} obtained for REF-52 and human aortic endothelial cells, yet again indicating that cells might feature the same scale of energy fluctuations in different settings. Similar to "*energy fluctuations of a single cell moving inside an aggregate of other cells*", we stress here as well that the literature measurements and analysis of cell sorting in a mixture of two cell-type aggregates briefly mentioned here invoked an equilibrium-like relation (where the ordinary temperature is replaced by an effective temperature T_{eff}) based on an analogy to two immiscible fluids at thermal equilibrium. No such equilibrium-like relations have been invoked in our own analyses discussed in "*cell-scale orientational fluctuations of noninteracting cells under periodic forcing*" and "*adhesion-scale contractile energy fluctuations of stationary adherent cells*".

DISCUSSION

The results presented in this letter indicate that active cellular fluctuations of adherent cells can be systematically quantified in various biophysical settings. Such analyses can provide quantitative information about the statistical distributions of relevant biophysical observables and an estimate of an effective temperature T_{eff} as a quantifier of a characteristic energy scale. The latter is found to be many orders of magnitude larger than the ordinary thermal energy scale, reflecting both the out-of-equilibrium, active nature of the fluctuations and the relatively large energy scales associated with cellular adhesion structures.

We find that various cell types under different biophysical conditions and observables being probed are characterized by a characteristic energy scale of fluctuations of $T_{\text{eff}} \sim 10^8$ K, i.e., about six orders of magnitude larger than room temperature. Yet, we also find that another cell type—which is known to exhibit dramatically different intrinsic temporal dynamics associated with its adhesions during cellular reorientation—features a characteristic energy scale of fluctuation of $T_{\text{eff}} \sim 10^{10}$ K. This significantly larger T_{eff} suggests that cell-type dependence cannot be generally excluded. Furthermore, we show that when adhesion structures and contractile forces are significantly weaker, as in the cancerous cells considered in Fig. 2 *e*, a much smaller T_{eff} emerges.

These findings call for extracting the energy scale of active fluctuations over a broader range of cell types, experimental settings and biophysical observables, and for understanding the biophysical origin and significance of such cellular energy scales. Once done, it may be possible to develop a better understanding of the collective spatiotemporal dynamics of adherent cells interacting with an extracellular matrix and

among themselves. Another interesting direction for future investigation, which goes beyond the scope of the present letter, is whether the results presented above might be useful in the possible development of a generalized (effective) statistical thermodynamics of adherent cells (18).

AUTHOR CONTRIBUTIONS

E.B. and A.M. conceptualized and designed the research, A.M. and H.W. performed the research, and all authors contributed to writing the manuscript.

ACKNOWLEDGMENTS

We are grateful to Sam Safran for urging us to compare the energy scale of active fluctuations across different biophysical settings. We are grateful to Ariel Livne for stimulating discussions and for providing most useful comments on the manuscript. We thank Lea Feld for her earlier contribution to the experiments that led to the data presented in "*adhesion-scale contractile energy fluctuations of stationary adherent cells*". This publication was partially made possible through the support of grant 62568 from the John Templeton Foundation (the opinions expressed in this publication are those of the authors and do not necessarily reflect the views of the John Templeton Foundation). E.B. acknowledges support from the Ben May Center for Chemical Theory and Computation and the Harold Perlman Family. H.W. acknowledges support from the Israel Science Foundation and from the Rappaport Family Foundation. H.W. is an incumbent of the David and Inez Myers Career Advancement Chair in Life Sciences.

DECLARATION OF INTERESTS

The authors declare no competing interests.

REFERENCES

1. Wang, H., W. Ip, R. Boissy, and E. S. Grood. 1995. Cell orientation response to cyclically deformed substrates: experimental validation of a cell model. *J. Biomech.* 28:1543–1552.
2. Wang, J. H., and E. S. Grood. 2000. The strain magnitude and contact guidance determine orientation response of fibroblasts to cyclic substrate strains. *Connect. Tissue Res.* 41:29–36.
3. Jungbauer, S., H. Gao, …, R. Kemkemer. 2008. Two characteristic regimes in frequency-dependent dynamic reorientation of fibroblasts on cyclically stretched substrates. *Biophys. J.* 95:3470–3478.
4. Faust, U., N. Hampe, …, R. Merkel. 2011. Cyclic stress at mhz frequencies aligns fibroblasts in direction of zero strain. *PLoS One.* 6:e28963.
5. Wang, J. H., P. Goldschmidt-Clermont, …, F. C. Yin. 2001. Specificity of endothelial cell reorientation in response to cyclic mechanical stretching. *J. Biomech.* 34:1563–1572.
6. Lin, J., X. Li, J. Yin, and J. Qian. 2020. Effect of cyclic stretch on neuron reorientation and axon outgrowth. *Front. Bioeng. Biotechnol.* 8:597867.
7. Mao, T., Y. He, Y. Gu, …, J. Ding. 2021. Critical frequency and critical stretching rate for reorientation of cells on a cyclically stretched polymer in a microfluidic chip. *ACS Appl. Mater. Interfaces.* 13:13934–13948.
8. Dai, Z.-X., P.-J. Shih, …, I.-J. Wang. 2022. Effect of static and dynamic stretching on corneal fibroblast cell. *Processes.* 10:605.
9. Livne, A., E. Bouchbinder, and B. Geiger. 2014. Cell reorientation under cyclic stretching. *Nat. Commun.* 5:3938.
10. Moriel, A., A. Livne, and E. Bouchbinder. 2022. Cellular orientational fluctuations, rotational diffusion and nematic order under periodic driving. *Soft Matter.* 18:7091–7102.
11. Kemkemer, R., C. Neidlinger-Wilke, …, H. Gruler. 1999. Cell orientation induced by extracellular signals. *Cell Biochem. Biophys.* 30:167–192.
12. Loy, N., and L. Preziosi. 2021. A statistical mechanics approach to describe cell re-orientation under stretch. Preprint at arXiv. https://doi.org/10.48550/arXiv.2108.00894.
13. Safran, S. A., and R. De. 2009. Nonlinear dynamics of cell orientation. *Phys. Rev. E Stat. Nonlin. Soft Matter Phys.* 80:060901.
14. Feld, L., L. Kellerman, …, H. Wolfenson. 2020. Cellular contractile forces are nonmechanosensitive. *Sci. Adv.* 6:eaaz6997.
15. Calzado-Martín, A., M. Encinar, …, A. San Paulo. 2016. Effect of actin organization on the stiffness of living breast cancer cells revealed by peak-force modulation atomic force microscopy. *ACS Nano.* 10:3365–3374.
16. Mombach, J. C., and J. A. Glazier. 1996. Single cell motion in aggregates of embryonic cells. *Phys. Rev. Lett.* 76:3032–3035.
17. Beysens, D. A., G. Forgacs, and J. A. Glazier. 2000. Cell sorting is analogous to phase ordering in fluids. *Proc. Natl. Acad. Sci. USA.* 97:9467–9471.
18. Schwarz, U. 2007. Soft matters in cell adhesion: rigidity sensing on soft elastic substrates. *Soft Matter.* 3:263–266.